



CT

1

: CT
 : 32 가
 17 , 6 , 5 , , ,
 1 . CT 3 ml 90 ml , , 30
 120 , 가 ,
 : CT
 : 가 , 17
 (100%) , 6 (100%)
 , 5 (100%) 가 .
 17 (100%) , 5 (100%)
 가 , 6 4 (66.7%)
 , CT
 (p<0.05).
 : CT
 CT

(1). CT 가 가 14:18, 43 (17 -70) . 17
 , 6 , 5 , ,
 가 , 가 , 1 .
 CT 3ml 90 ml
 (2). iopamidol (Iopamiro 300; Bracco, Milan, Italy)
 CT (HiSpeed
 Advantage; GE Medical Systems, Milwaukee, U.S.A.)
 (3-5). , 30 120 35
 . 35 (acqui-
 sition time), 5 mm collimation, 5 mm

CT
 6.5 - 20 (11)
 가 Mann - Whitney test
 CT Friedman test , p
 0.05
 가
 CT
 가 1 (Table 1).
 (window width, 240 HU) (level, 20 HU)
 CT
 CT (Hounsfield units)
 가
 CT (20 - 70 mm²)
 17 (100%) (Fig. 1),
 5 (100%) 가 (Fig. 2).
 6 (100%)
 (Fig. 3).
 17 (100%) 5
 3 (60%) 가 . , 5 2

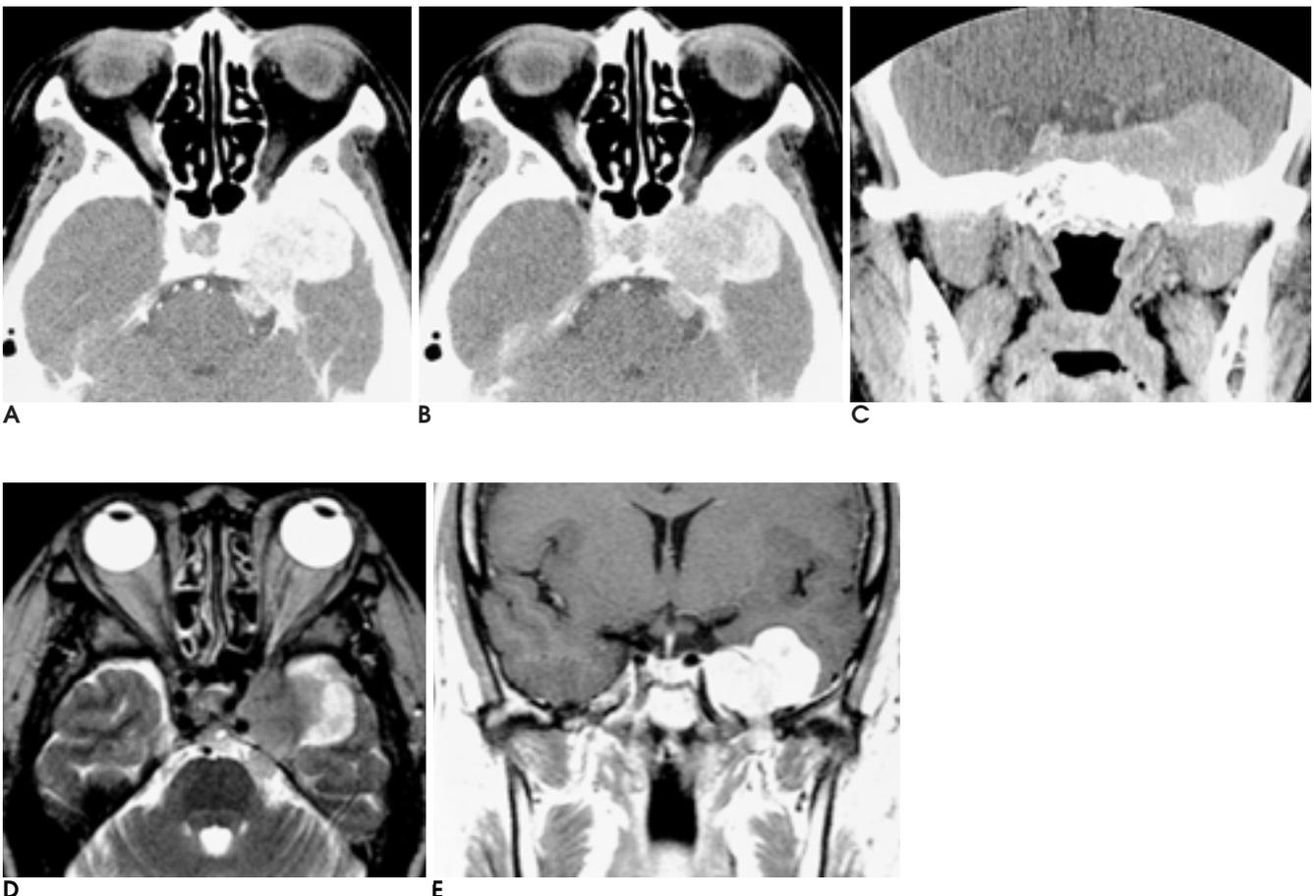


Fig. 1. A 44-year-old woman with parasellar meningioma.
A. Axial early phase scan shows strong enhancement of the mass in the left parasellar area that invades Meckel's cave.
B. Axial late phase scan shows decrease in attenuation of the mass.
C. Coronal scan shows further decrease in attenuation of the mass that extends into the skull base through the foramen ovale.
D. Axial T2-weighted MR scan shows isointense mass with peripheral hyperintense signal.
E. Coronal postcontrast T1-weighted MR scan shows strong enhancement of the mass that extends into skull base through the foramen ovale. MR features of the mass are similar to those of neurogenic tumors.

Table 1. Visual Assessment of Attenuation Changes of Various Tumors on Two-phase Helical CT Scans

	No. of tumors	Change in attenuation								
		Early and delayed*			Delayed and coronal			Early and coronal		
		D ⁺	N	I	D	N	I	D	N	I
Meningioma	17	17	0	0	17	0	0	17	0	0
Neurogenic tumor	5	0	0	5	0	2	3	0	0	5
Pituitary macroadenoma	6	0	6	0	2	4	0	2	4	0
Cavernous angioma	1	0	0	1	0	0	1	0	0	1
Chondrosarcoma	1	0	0	1	0	0	1	0	0	1
Osteosarcoma	1	0	0	1	1	0	0	0	0	1
Sphenoid carcinoma	1	0	1	0	1	0	0	1	0	0

*Early = early phase transverse scan, Delayed = delayed phase transverse scan, Coronal = coronal scan

⁺D = decreased, N = no change, I = increased.



Fig. 2. A 68-year-old man with parasellar Schwannoma.

A. Axial early phase scan shows dumbbell shaped mass in the right parasellar area. There is mild enhancement of the mass except for the non-enhancing peripheral cystic portion.

B, C. Axial delayed phase scan (**B**) and coronal scan (**C**) show increased enhancement of the mass that extends into the skull base through the foramen ovale.



Fig. 3. Pituitary macroadenoma in a 30-year-old man.

A. Axial early phase scan shows homogenous moderate enhancement of the mass at the right sella, cavernous sinus, and Meckel's cave.

B, C. Axial late phase (**B**) and coronal scan (**C**) shows no significant change in attenuation of the mass.



Fig. 4. A 56-year-old woman with parasellar cavernous angioma.
A. Axial early phase scan shows peripheral nodular enhancement of the mass.
B. Axial late phase scan shows central filling-in enhancement of the mass.
C. Coronal delayed scan shows homogenously strong enhancement of the mass that is similar to a meningioma.

Table 2. CT Numbers and Ratios of CT Numbers of Various Tumors at Each Phase on Two-phase Helical CT Scan

	CT number*			Ratio	
	Early [†]	Delayed	Coronal	Delayed/Early	Coronal/Early
Meningioma	105.0 ± 38.7	81.4 ± 22.1	59.5 ± 13.2	0.80 ± 0.11	0.60 ± 0.12
Neurogenic tumor	49.8 ± 11.5	64.8 ± 6.3	71.4 ± 5.3	1.34 ± 0.22	1.50 ± 0.38
Pituitary macroadenoma	64.5 ± 12.3	64.2 ± 13.0	58.5 ± 6.7	0.97 ± 0.08	0.89 ± 0.14
Cavernous angioma	60	80	90	1.33	1.5
Chondrosarcoma	35	55	107	1.57	3.06
Osteosarcoma	67	99	75	1.48	1.12
Sphenoid carcinoma	86	85	80	0.99	0.93

*Data are the mean ± SD.

[†]Early = early phase transverse scan, Delayed = delayed phase transverse scan, Coronal = coronal scan

(40%) 6 4 (66.7%)
 .
 17 (100%) , 5
 (100%) 가 , 6 4
 (66.7%)
 가,
 4). 1 (Fig.

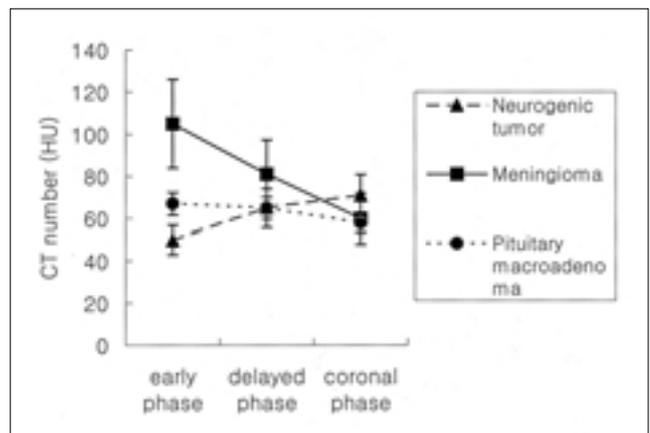


Fig. 5. Time-attenuation curves for meningiomas(n=17), neurogenic tumor(n=5), and pituitary macroadenomas(n=6). Meningiomas show a strong enhancement at early phase with a decrease of attenuation at delayed phase and coronal scans, while schwannomas show a pattern of delayed enhancement. In pituitary macroadenomas, the degree of enhancement show no significant change among three phases. Error bars indicate SDs.

CT
 (p=0.001, p=0.039) (Table 2).

CT
 (p=0.000, p=0.003),

(p=0.082).

CT

($p=0.031, p=0.004$),

($p=0.865$).

CT

($p=0.062$).

CT

CT

14 (82.4%)

CT

17

($p=0.000, p=0.000$).

80 HU

CT

80 HU

CT

CT

0.80

0.60

1

CT

가

(12).

CT

1.34

1.50

1

가

가

가

가

(12 - 17).

0.89 1 가

CT

0.97

(Fig. 5).

Takeda (14)

, Takeda (14)

가

가

가

가 가

(2).

가

CT

가

(6).

가

(18, 19),

CT

(7-

CT

가

CT

9),

(9, 16, 17, 20, 21),

CT

가 . MRI

CT

가

가 (6).

가

가

가 가

(6, 10).

CT

CT

가

)

CT

CT

CT

CT MRI

(3, 11).

CT

CT

1. Tanohata K, Maehara T, Aida N, et al. Computed tomography of intracranial chondroma with emphasis on delayed contrast enhancement. *J Comput Assist Tomogr* 1987;11:820-823
2. Wiot JG. Radiologic evaluation of the skull base. *Ear Nose Throat J* 1991;70:563-576
3. Choi DS, Na DG, Byun HS, et al. Salivary gland tumors: Evaluation with two-phase helical CT. *Radiology* 2000;214:231-236
4. Choi BI, Lee HJ, Han JK, Choi DS, Seo JB, Han MC. Detection of hypervascular nodular hepatocellular carcinomas: Value of triphasic helical CT compared with iodized-oil CT. *AJR Am J Roentgenol* 1997;168:219-224
5. Ryoo JW, Na DG, Woo JY, et al. Investigation of juxtaseilar and cerebellopontine angle meningio-mas and neurogenic tumors: two-phase helical CT. *Neuroradiology*, 2001;43:637-643
6. Johnsen DE, Woodruff WW, Allen IS, Cera PJ, Funkhouser GR, Coleman LL. MR imaging of the sellar and juxtaseilar regions. *RadioGraphics* 1991;11:727-758
7. Moore T, Ganti SR, Mawad ME, Hilal SK. CT and angiography of primary extradural juxtaseilar tumors. *AJR Am J Roentgenol* 1985; 145:491-496
8. McCormick PC, Bello JA, Post KD. Trigeminal schwannoma: Surgical series of 14 cases with review of the literature. *J Neurosurg* 1988;69:850-860
9. Abrahams JJ, Eklund JA. Diagnostic radiology of the cranial base. *Clin Plast Surg* 1995;22:373-405
10. Catz A. and Reider-Groswasser. Acoustic neurinoma and posterior fossa meningioma. clinical and CT radiologic findings. *Neuroradiology* 1986;28:47-52
11. Suojanen JN, Mukherji SK, Dupuy DE, Takahashi JH, Costello P. Spiral CT in evaluation of head and neck lesion: Work in progress. *Radiology* 1992;183:281-283
12. Som PM, Lanzieri CF, Sacher M, Lawson W, Biller HF. Extracranial tumor vascularity: Determination by dynamic CT scanning. II. the unit approach. *Radiology* 1985;154:407-412
13. Michael AS, Mafee MF, Valvassori GE, Tan WS. Dynamic computed tomography of the head and neck: Differential diagnostic value. *Radiology* 1985;154:413-419
14. Takeda N, Tanaka R, Nakai O, Ueki K. Dynamics of contrast enhancement in delayed computed tomography of brain tumors: Tissue-blood ratio and differential diagnosis. *Radiology* 1982;142: 663-668
15. Binger DD, McLwndon RE, Bruner JM. *Russell and Rubinstein's pathology of tumors of the nervous system*. Arnold, London, 1998;67-193
16. Wu EH, Tang YS, Zhang YT, Bai RJ. CT in diagnosis of acoustic neuromas. *AJNR Am J Neuroradiol* 1986;7:645-650
17. MR CT . 1998; 38: 221-228
18. Adam IL, John MT, Troy DP, et al. Dural cavernous angiomas outside the middle cranial fossa: A report of two cases. *Neurosurg* 1994;35:498-504
19. Quinn SF, Benjamin GG. Hepatic cavernous hemangiomas: Simple diagnosis sign with dynamic bolus CT. *Radiology* 1992;182: 545-548
20. Bahr AL, Gayler BW. Cranial chondrosarcomas: Report of four cases and review of the literature. *Radiology* 1977;124:151-156
21. Grossman RI, Davis KR. Cranial computed tomographic appearance of chondrosarcoma of the base of the skull. *Radiology* 1981; 141:403-408

Analysis of Enhancement Pattern of Sellar and Parasellar Tumors Using Two-Phase Helical CT¹

Ji Young Woo, M.D., Jae Wook Ryoo, M.D., Dong Gyu Na, M.D.,
Hong Gee Roh, M.D., Hong Sik Byun, M.D.

¹Department of Radiology, Samsung Medical Center, Sungkyunkwan University College of Medicine

Purpose: To assess the enhancement patterns of sellar and parasellar tumors at two-phase helical CT.

Materials and Methods: Thirty-two patients with pathologically proven sellar and parasellar tumors [meningioma (n=17), pituitary macroadenoma (n=6), neurogenic tumor (n=5), cavernous angioma (n=1), chondrosarcoma (n=1), osteosarcoma (n=1), sphenoid carcinoma (n=1)] were included in this study. Two-phase helical CT was performed after the injection of 90 mL of contrast material at a rate of 3 mL/sec. Transverse helical CT scans were obtained during the early and late phases, with scanning delays of 30 and 120 seconds, respectively. Delayed coronal images were obtained after delayed axial images. Attenuation change and the enhancement patterns of the tumors were visually assessed; the former was also assessed quantitatively as the ratio of the CT number at late-phase axial and coronal scanning to that at early-phase scanning.

Results: Visual assessment of two-phase helical CT images revealed decreased attenuation in all 17 meningiomas, no change in all six pituitary macroadenomas and increased attenuation in 5 all five neurogenic tumors on late-phase axial scans as compared with early phase scans. Coronal images showed decreased attenuation in all 17 meningiomas, increased attenuation in all five neurogenic tumors and no change in four pituitary macroadenomas (66.7%). The ratio of CT numbers was significantly different between meningiomas, neurogenic tumors and pituitary macroadenomas ($p < 0.05$).

Conclusion: According to their histopathology, sellar and parasellar tumors showed characteristic enhancement patterns at two-phase helical CT. An analysis of the observed enhancement patterns can be useful in the differential diagnosis of juxtaseellar tumors.

Index words : Computed tomography (CT), helical technology
Skull, base
Skull, primary neoplasms

Address reprint requests to : Jae Wook Ryoo, M.D., Department of Radiology, Samsung Medical Center,
Sungkyunkwan University College of Medicine, 50 Ilwon-dong, Kangnam-gu, Seoul 135-710, Korea.
Tel. 82-2-3410-0519 Fax. 82-2-3410-0084 E-mail: ryoojw@smc.samsung.co.kr